s- and p-wave neutrons on ^{30}Si and ^{34}S: Spherical optical model analysis

R. F. Carlton

Middle Tennessee State University, Murfreesboro, Tennessee 37132

J. A. Harvey and C. H. Johnson

Oak Ridge National Laboratory, Oak Ridge, Tennessee 37831

The s- and p-wave neutron scattering functions obtained previously by R-matrix analyses of high resolution transmission data for 0–1.4 MeV neutrons on ^{30}Si and ^{34}S have been averaged by means of a simple analytic approximation to obtain experimental optical model scattering functions. To describe these with a spherical optical model potential requires the real well depth to be about 20% deeper for p waves than for s waves. This result agrees with an earlier analysis for ^{32}S and suggests that deformation effects must be included for all three nuclei.

I. INTRODUCTION

The phenomenological optical model potential (OMP) has been used[1] extensively to describe data on average nucleon scattering functions. Most such data involve sums over many partial waves for incident nucleon energies of several MeV. However, by scattering neutrons at lower energies where good energy resolution is possible, one can measure the scattering function for each significant partial wave and then, by subsequent averaging over energy, deduce an OMP for the individual partial waves. For neutron energies less than about 10 keV there is already an extensive body of data[2] on average s-wave scattering functions. These results are usually expressed in terms of a radius R' and a strength function $\langle \Gamma_n^0 \rangle / D$. However, few analyses have been made in the energy range of several hundred keV where high resolution neutron experiments are possible and where a few partial waves higher than s waves become important.

From high resolution neutron data[3] on ^{32}S and the corresponding scattering functions, Johnson and Winters[4,5] deduced average scattering functions for s and p waves in the energy region from 0 to 1.1 MeV. To fit those averages with a spherical OMP required a real well 20% deeper for p waves than for s waves. MacKellar and Castel[6] showed that this difference can be attributed to the deformation of the ^{32}S target. (Recently, MacDonald[7] also deduced an OMP from the ^{32}S resonance parameters[3] by a different averaging procedure than Refs. 4 and 5.)

One can reasonably expect other deformable nuclei near ^{32}S to require a similar l dependence for the spherical OMP. Here we extend the OMP analysis to ^{30}Si and ^{34}S transmission data that were obtained[8,9] at ORELA, the same time-of-flight facility as used previously for ^{32}S. Since relatively small enriched samples of ^{30}Si and ^{34}S had to be used, it was necessary to restrict the neutron beam and to use a shorter flight path than for ^{32}S. As a result the statistical uncertainties for ^{30}Si and ^{34}S are larger and the energy resolutions poorer than for ^{32}S. Nevertheless, the following analysis shows there is enough information to demonstrate an l dependence of the spherical OMP.

Since few resonances are observed for these nuclei, the width of the averaging functions must be comparable to the energy range of the measurements in order to average over several resonances. The earlier analysis by Johnson and Winters[4,5] for ^{32}S used an approximate procedure equivalent to the use of a very broad averaging function. At that time, however, that procedure had been justified[10,11] only for nuclei with level spacing D small enough such that the width of the averaging function can be made much larger than D but still much narrower than the region of measurements. Those conditions do not hold for these nuclei. Recently, Johnson, Larson, Mahaux, and Winters[12] (hereafter called JLMW) reviewed the relationship of the averaged experimental scattering function to the OMP and showed numerically that very broad averaging functions are valid. Furthermore, averaging can be done approximately by a simple procedure; in fact the method used previously[4,5] for ^{32}S is a good approximation for very large averaging widths.

In Sec. II we review the averaging procedure. In Secs. III and IV we find average scattering functions for ^{30}Si and for ^{34}S, and in Sec. V we fit these functions with a spherical OMP. Section VI is our summary.

II. AVERAGING OF THE SCATTERING FUNCTION

This section is a summary of pertinent equations from JLMW.[12] We discuss only spin-zero targets and relatively broad resonances, for which only the entrance neutron channel is important. For a given J^π the cross section is related to the real part S_r of the scattering function,

$$\sigma(E) = 2\pi k^{-2} g_J [1 - S_r(E)] , \qquad (1)$$

where k is the neutron wave number and g_J is the statistical factor, $J + \frac{1}{2}$. Given S_r, one can find also the imaginary part of S because S is unitary.

To fit the data we expand S in terms of the R function of the R matrix formalism, which automatically embodies the unitary property. In the one-open-channel case we have for a given J^π

$$S(E) = e^{-2i\phi(E)} \frac{1 + iP(E)R(E)}{1 - iP(E)R(E)} , \qquad (2)$$

where ϕ is the hard-sphere phase shift and P is the penetrability. The functions, ϕ, P, and R depend on the chosen boundary radius a. In writing Eq. (2) we have chosen the boundary parameter B of the formalism to be equal to the shift function.

The R function is a sum over all levels both inside and outside of the region of measurements but it can be written explicitly only for the N resonances actually observed within the region. Thus, we write

$$R(E) = \sum_{\lambda=1}^{N} \gamma_\lambda^2/(E_\lambda - E) + R^{\text{ext}}(E) , \qquad (3)$$

where E_λ and γ_λ^2 are the energies and reduced widths of the observed levels, and where R^{ext} is defined within the region to account for the effects of the external levels. In the fitting procedure the γ_λ^2 and E_λ are free resonance parameters and the R^{ext} is a parametric function used to fit the off-resonance cross sections and the interference patterns.

Since R^{ext} must increase smoothly with energy within the region, it could be parametrized in various simple forms. However, JLMW showed that a particular form is appropriate for the subsequent averaging of $S(E)$. That form, which is the same as used for the ^{32}S analysis,[4,5] is

$$R^{\text{ext}}(E) = \widetilde{R}(E) - \tilde{s} \ln \frac{E_u - E}{E - E_l} , \qquad (4)$$

where E_l and E_u are the lower and upper energy limits of the measured region, $\widetilde{R}$ is a simple parametric function such as $\alpha + \beta E$, and $\tilde{s}$ is in the observed strength function,

$$\tilde{s} \equiv \langle \gamma^2 \rangle / D = \frac{\sum_{\lambda=1}^{N} \gamma_\lambda^2/N}{(E_N - E_1)/(N-1)} . \qquad (5)$$

Having obtained the experimental scattering function in parametric form, we can average for each J^π in order to compare with an OMP scattering function. We first factor the observed $S(E)$ into resonance and nonresonance components. The experimental optical model scattering function is then defined by an average over only the resonance part,

$$S^{\text{OM}}(E) \equiv S_{\text{bgr}}(E) \langle S_{\text{res}}(E) \rangle_I , \qquad (6)$$

where $2I$ is the width of the averaging function.

We could average numerically. In that case, the particular form chosen to parametrize R^{ext} would not be important. However, as JLMW showed, the above parametrization leads to a simple good approximation to the average,

$$S^{\text{OM}}(E) \simeq e^{-2i\phi(E)} \frac{1 + iP(E)[\widetilde{R}(E) + i\pi\tilde{s} + R^f(\mathscr{E})]}{1 - iP(E)[\widetilde{R}(E) + i\pi\tilde{s} + R^f(\mathscr{E})]} , \qquad (7)$$

where

$$R^f(\mathscr{E}) = \sum_{\lambda=1}^{N} \frac{\gamma_\lambda^2}{E_\lambda - \mathscr{E}} - \int_{E_l}^{E_u} \frac{\tilde{s} \, dE'}{E' - \mathscr{E}} . \qquad (8)$$

Here $\mathscr{E}$ is a complex energy, $E + iI$. Clearly, both the real and imaginary parts of R^f fluctuate about an average value of about zero. Furthermore, since R^f vanishes as I goes to infinity, a good approximation for large I is found

by omitting R^f in Eq. (7).

We have calculated approximate average experimental scattering functions by use of Eq. (7), both with and without R^f, and have compared the results with those from a spherical OMP. Various quantities[12] could be used to make a graphical comparison. Our choice, as in Ref. 5, is to plot quantities which are proportional to the shape elastic and compound nucleus cross sections,

$$\sigma_{\text{SE}}(E)/g_J = \pi k^{-2} |1 - S^{\text{OM}}(E)|^2 \qquad (9)$$

and

$$\sigma_c(E)/g_J = \pi k^{-2}(1 - |S^{\text{OM}}(E)|^2) . \qquad (10)$$

III. EXPERIMENTAL $S^{\text{OM}}(E)$ for ^{34}S

Carlton et al.[8] measured the transmission of 0.0—1.5 MeV neutrons on a target of sulfur enriched to 94.5% in ^{34}S and, from an R-matrix analysis for a 4.37-fm boundary radius, deduced resonance parameters and the corresponding $\langle \gamma^2 \rangle / D$ for *s*- and *p*-wave neutrons. To parametrize R^{ext} they used Eq. (4) with the approximation that $\widetilde{R}$ is linear. Figure 1 shows the $\widetilde{R}$ and R^{ext}. The observed difference between *s* waves and *p* waves for $\widetilde{R}$ is primarily responsible for the difference in real well depths discussed below; the average difference between $p_{1/2}$ and $p_{3/2}$ is evidence for the spin-orbit potential. The error bars, which are plotted only at the center of the experimental region, were estimated from various fits and indicate overall uncertainties across the whole region. The larger uncertainty for $p_{1/2}$ than for $p_{3/2}$ results because only one broad $p_{1/2}$ resonance with a distinctive resonance-potential interference pattern was observed.

Using $\widetilde{R}$ and the resonance parameters[8] γ_λ^2 and E_λ, we have calculated approximate average scattering functions using Eq. (7) both with and without R^f. Figures 2—4
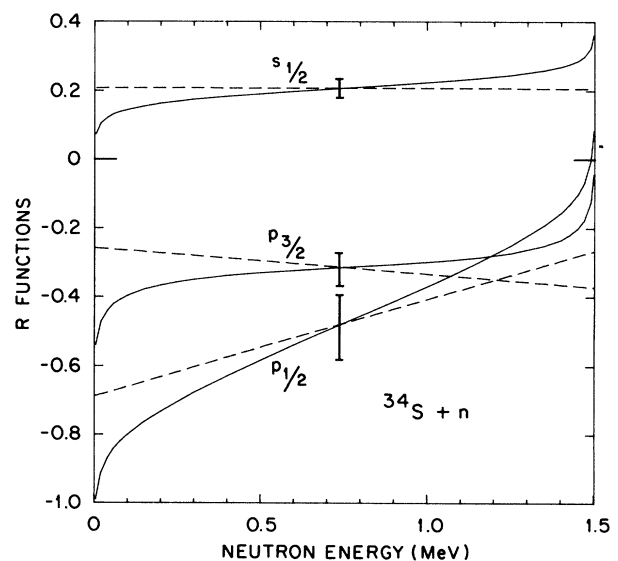

FIG. 1. The function $\widetilde{R}$ (dashed curves) and R^{ext} (solid curves) from the R-matrix analysis of n+^{34}S by Carlton et al. in Ref. 8. The error bars indicate overall uncertainties over the whole energy region.
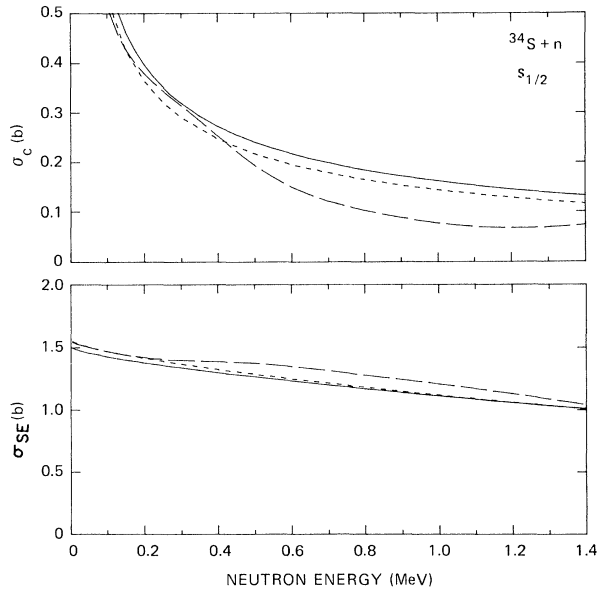
FIG. 2. Experimental and OMP shape elastic and compound cross sections for $s_{1/2}$ neutrons on ^{34}S. The long-dash curves are experimental values found from the approximate average of Eq. (7) for $I=300$ keV and the solid curve is that approximation with R^f omitted. The short-dash curves show a visual OMP fit with the parameters given in Table I.

show σ_{SE}/g_J and σ_c/g_J with R^f included for $I=300$ keV (long-dash curve) and with R^f omitted (solid curves). We note that the spread in the curves for these two approximations is larger for σ_c than for σ_{SE} because σ_c depends primarily on the resonance structure whereas σ_{SE} depends on the smoothly varying R^{ext}.

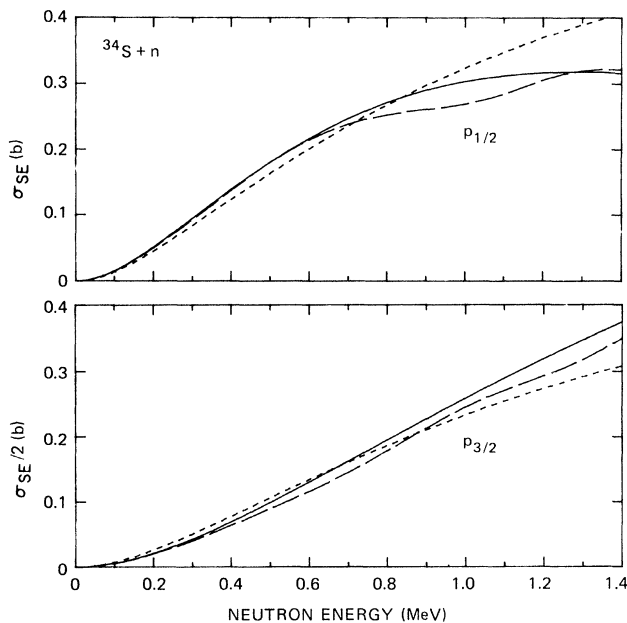We emphasize that the curves, which are plotted from 0

FIG. 3. Experimental and OMP shape elastic cross sections divided by g_J for p-wave neutrons on ^{34}S. For $p_{3/2}$ $g_J=2$ and for $p_{1/2}$ $g_J=1$. Curve symbols are as in Fig. 2.
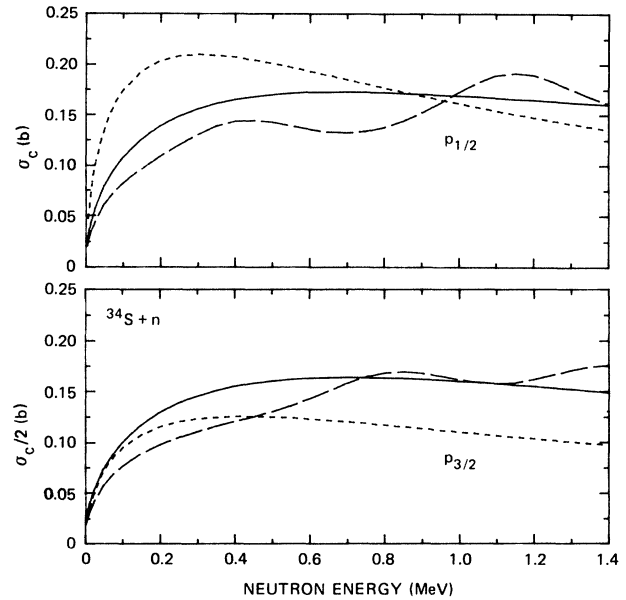

FIG. 4. Experimental and OMP compound cross sections divided by g_J for p-wave neutrons on ^{34}S. Curve symbols are as in Fig. 2.

to 1.4 MeV, were each obtained with very broad averaging functions. Thus, the detailed energy dependences are not very significant, particularly above 1 MeV, where the resonance structure was not fully resolved. Nevertheless the broad region of measurement was needed to show that R^{ext} is due to relatively distant levels, not to the accidental presence of nearby strong levels.
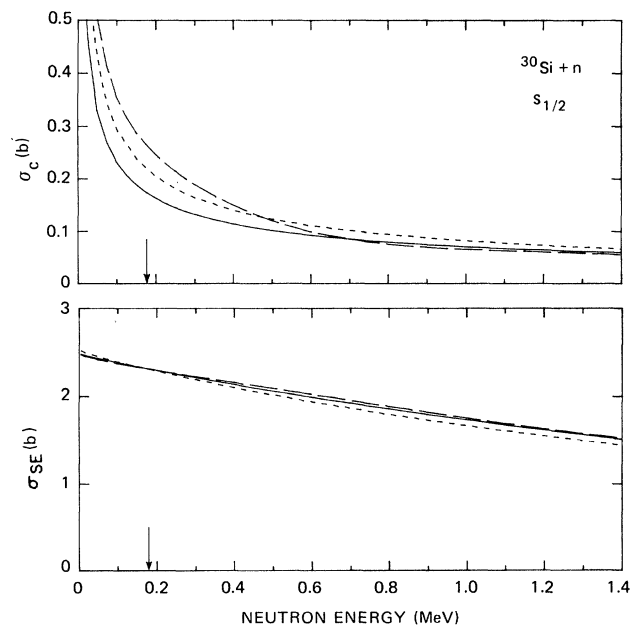

FIG. 5. Experimental and OMP shape elastic and compound cross sections for s-wave neutrons on ^{30}Si. Curve symbols are as in Fig. 2 except that $I=500$ keV for the long-dash curve. The arrow shows the energy of the resonance that provided the primary data for σ_{SE}.
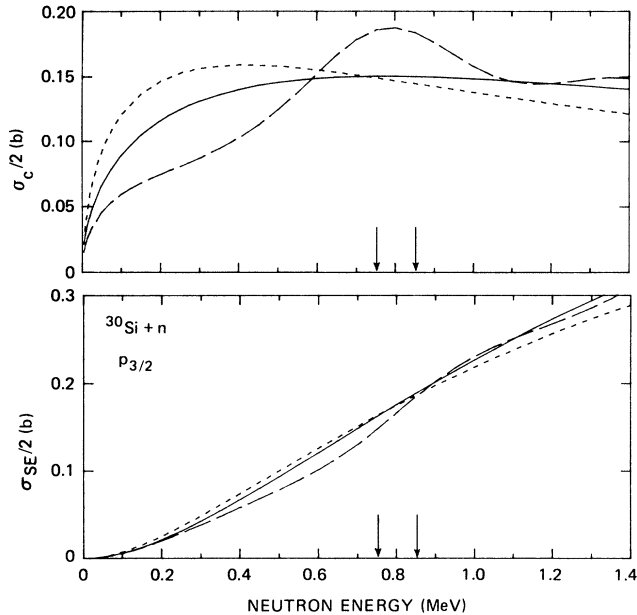
FIG. 6. Experimental and OMP shape elastic and compound cross sections divided by g_J for *p*-wave neutrons on ^{30}Si. Curve symbols are as in Fig. 2. Arrows show the energies of two resonances that provided the primary data for σ_{SE}.

IV. EXPERIMENTAL $S^{OM}(E)$ FOR ^{30}Si

Harvey *et al.*[9] measured the transmission of 0.0–1.4 MeV neutrons on ^{30}SiO$_2$ and made an *R*-matrix analysis similar to that for ^{34}S except that the boundary radius was 4.2 fm and the R^{ext} were parametrized by distant poles above and below the experimental region. Since the large cross section for oxygen in SiO$_2$ made it impossible to extract precise information on R^{ext} from the nonresonance cross sections, the essential information came from the potential-resonance interference patterns for a broad *s*-wave resonance at 183 keV and for two broad $p_{3/2}$ resonances at 745 and 845 keV. The information for $p_{1/2}$ neutrons was inadequate for the present analysis because no broad $p_{1/2}$ resonances were observed.

We converted their pole expansion for R^{ext} to the form of Eq. (4). For this purpose we use $\langle \gamma^2 \rangle /D$ for the full energy region from $E_l=0.0$ to $E_u=1.4$ MeV, but, since no significant information was obtained on the energy

dependence of R^{ext}, we parametrize $\tilde{R}$ simply as constant. Thus, we find $\tilde{R}=-0.06\pm0.05$ and -0.35 ± 0.10, respectively, for the $s_{1/2}$ and $p_{3/2}$ channels.

Figures 5 and 6 show σ_{SE} and σ_c calculated using $\tilde{R}$ and the reported[9] strength functions; the $S^{OM}(E)$ were calculated from Eq. (7) with R^f included for the long-dash curves and omitted for the solid curves. With R^f included we used $I=500$ keV for $s_{1/2}$ and $I=300$ keV for $p_{3/2}$. Each curve is plotted from 0 to 1.4 MeV; however, arrows are included to indicate the positions of the broad resonances which provided the essential data on R^{ext}, and hence on σ_{SE}. Again we emphasize that the broad region was needed to show that R^{ext} is due to relatively distant levels, not to the accidental presence of a nearby strong level.

V. SPHERICAL OPTICAL MODEL POTENTIAL

Following the previous procedure[5] for ^{32}S we use here a Woods-Saxon form factor for the real potential and Woods-Saxon derivatives for the spin-orbit and imaginary potentials. As previously, we fixed $r_0=1.21$ fm, $a_0=0.66$ for the real wells, and $a_D=0.48$ fm for the imaginary well. We then adjusted the well depths V_0, V_{so}, and W_D to obtain the best visual fits to the experimental averages. These fits are the short-dash curves in Figs. 2–6. For ^{34}S *p* waves we adjusted V_{so} to fit σ_{SE} for both $p_{1/2}$ and $p_{3/2}$ but allowed only a single value of W_D for fitting σ_c. For ^{30}Si, for which $p_{1/2}$ curves are not available, we assumed $V_{so}=7\pm3$ MeV. In obtaining the visual fits we emphasized energy regions judged to be most experimentally reliable.

Table I lists the fitted well depths not only for ^{30}Si and ^{34}S but also for ^{32}S from Ref. 5. The uncertainties for ^{30}Si and ^{34}S are those propagated from uncertainties on $\tilde{R}$ and $\langle \gamma^2 \rangle /D$. Uncertainties in $\langle \gamma^2 \rangle /D$ were assigned[8,9] from the fluctuations in Porter-Thomas widths and Wigner spacings whereas, as indicated above, the uncertainties in $\tilde{R}$ were estimated from various fits to the data. For ^{30}Si the assumed uncertainty in V_{so} is also propagated. For ^{32}S the uncertainties are from Ref. 4. Qualitatively, the uncertainty in $\tilde{R}$ propagates to V_0 and V_{so}, whereas the uncertainty in $\langle \gamma^2 \rangle /D$ propagates to W_D.

VI. CONCLUSION

An examination of the spherical OMP well depths in Table I for the nuclei ^{30}Si, ^{32}S, and ^{34}S shows that, con-

TABLE I. Spherical optical model potential parameters. Geometric parameters $r_0=r_D=1.21$ fm, $a_0=0.66$ fm, and $a_D=0.48$ fm. See text.

Target	*l*	V_0 (MeV)	V_{so} (MeV)	W_D (MeV)
^{30}Si	0	48 ±1.7		2.0^{+2}_{-1}
	1	62 ±2.5	$(7\pm3)^a$	4.5^{+3}_{-2}
^{32}S	0	51.5±0.4		$6.0^{+4}_{-2.5}$
	1	61.4±1.1	11±3	2.7±1.5
^{34}S	0	51.5±1.1		$3.0^{+3}_{-1.1}$
	1	58.5±1.2	6±3.5	3.5±1.9

^{a}Assumed value.

sistent with the assigned uncertainties, the imaginary depth W_D is about the same for all three nuclei. Also, the three values of V_0 for s waves are comparable as are the three values of V_0 for p waves. But V_0 for p waves is clearly deeper than for s waves. The average of the three values, weighted inversely with their variances, is $V_0 = 51.3$ MeV for s waves and $V_0 = 60.3$ MeV for p waves; these differ by 18%.

We conclude that the phenomenological spherical OMP is appropriate in this mass region in the sense that it can be parametrized to give a systematic description of the three nuclei. In that regard it would be interesting to extend this study to other nearby nuclei. On the other hand, the requirement for an l dependence in V_0 suggests that the spherical model is not adequate. For ^{32}S MacKellar

and Castel[6] have already shown that the l dependence can be alleviated if the proper dynamic deformation of the target nucleus is introduced. One expects the same to be true for ^{30}Si and ^{34}S, since these nuclei have similar deformations. In the companion paper[13] MacKellar and Castel treat these deformations.

ACKNOWLEDGMENTS

[1]C. M. Perey and F. G. Perey, At. Data Nucl. Data Tables 17, 1 (1976).

[2]S. F. Mughabghab, M. Divadeenam, and N. E. Holden, *Neutron Cross Sections* (Academic, New York, 1981), Vol. 1, Part A.

[3]J. Halperin, C. H. Johnson, R. R. Winters, and R. L. Macklin, Phys. Rev. C 21, 545 (1980).

[4]C. H. Johnson and R. R. Winters, Phys. Rev. C 21, 2190 (1980).

[5]C. H. Johnson and R. R. Winters, Phys. Rev. C 27, 416 (1983). Correction: The labels on the ordinate of Fig. 2 should be 0.5, 1.0, and 1.5 rather than 1, 2, and 3.

[6]A. D. MacKellar and B. Castel, Phys. Rev. C 28, 441 (1983).

[7]W. M. MacDonald, Nucl. Phys. A395, 221 (1983).

[8]R. F. Carlton, W. M. Good, J. A. Harvey, R. L. Macklin, and B. Castel, Phys. Rev. C 29, 1980 (1984).

[9]J. A. Harvey, W. M. Good, R. F. Carlton, B. Castel, J. B. McGrory, and S. F. Mughabghab, Phys. Rev. C 28, 24 (1983).

[10]A. M. Lane and R. G. Thomas, Rev. Mod. Phys. 30, 257 (1958).

[11]J. E. Lynn, *The Theory of Neutron Resonance Reactions* (Clarendon, Oxford, 1968).

[12]C. H. Johnson, N. M. Larson, C. Mahaux, and R. R. Winters, Phys. Rev. C 27, 1913 (1983).

[13]A. D. MacKellar and B. Castel, Phys. Rev. C 29, 1993 (1984), the following paper.